Progressive Inter-carrier Interference Equalization for OFDM Transmission over Time-varying Underwater Acoustic Channels

Jianzhong Huang, *Student Member, IEEE,* Shengli Zhou, *Member, IEEE,* Jie Huang, Christian R. Berger, *Member, IEEE,* and Peter Willett, *Fellow, IEEE*

***Abstract*—Multicarrier modulation in the form of orthogonal-frequency-division-multiplexing (OFDM) has been intensively pursued for underwater acoustic (UWA) communications recently due to its ability to handle long dispersive channels. Fast variation of UWA channels destroys the orthogonality of the sub-carriers and leads to inter-carrier interference (ICI), which degrades the system performance significantly. In this paper we propose a progressive receiver dealing with time-varying UWA channels. The progressive receiver is in nature an iterative receiver, based on the turbo principle. However, it distinguishes itself from existing iterative receivers in that the system model for channel estimation and data detection is itself continually updated during the iterations. When the decoding in the current iteration is not successful, the receiver increases the span of the ICI in the system model and utilizes the currently available soft information from the decoder to assist the next iteration which deals with a channel with larger Doppler spread. Numerical simulation and experimental data collected from the *2008 Surface Processes and Acoustic Communications Experiment* (SPACE08) show that the proposed receiver can self adapt to channel variations, enjoying low complexity in good channel conditions while maintaining excellent performance in adverse channel conditions.**

***Index Terms*—Turbo equalization, iterative receiver, sparse channel estimation, OFDM, inter-carrier interference, underwater acoustic communications.**

I. Introduction

Recently, multicarrier modulation in the form of orthogonal-frequency-division-multiplexing (OFDM) has been actively pursued for underwater acoustic communications; see performance results based on data recorded from various field experiments in [2]–[13]. Different receivers are built based on different assumptions on the underlying channel models. Specifically, the receivers in [2]–[10] assume that inter-carrier interference (ICI) can be neglected after proper resampling and Doppler shift compensation, while the receivers in [11]–[13] explicitly deal with ICI. Ignoring the ICI, the receivers in [2]–[9] have low complexity on channel estimation and data detection, however, their performance degrades quickly in channels with large Doppler spread. Explicitly accounting for the ICI, the receiver in [13] achieves robust performance even in very challenging channel conditions. However, it requires a significant pilot overhead for channel estimation, and the receiver complexity is considerably higher than its ICI-ignorant counterparts [16].

In practice, underwater acoustic (UWA) channels are rapidly time-varying due to environmental variations such as wind speed, wave height, and the motion of the transceiver platforms. So far, there is no commonly-agreed model for UWA channels. One important area of research is to investigate how environmental factors affect the performance of a particular receiver structure, see e.g., [17], [18].

In this paper, we propose an OFDM receiver that can adapt to different channel conditions in an automatic fashion. By its nature, the proposed progressive receiver is an iterative receiver, following the turbo principle. However, it distinguishes itself from existing iterative receivers, e.g., [19]–[25], in that the system model itself for channel estimation and data detection keeps being updated during the iterations. When the decoding in the current iteration is not successful, the receiver increases the span of the ICI in the system model and utilizes the available soft information from the channel decoder to deal with a channel with a larger Doppler spread in the next iteration.

For channel estimation, we use basis pursuit algorithms developed in the compressed sensing context to exploit the sparse nature of UWA channels [13], where we also incorporate the soft information from the decoder. The ICI mitigation problem in the frequency-domain is equivalent to that of intersymbol interference (ISI) equalization in the time-domain, but with time-varying ISI coefficients. Hence, existing methods for ISI equalization can be directly used for ICI mitigation. In this paper, we adopt the maximum *a posteriori* (MAP) equalizer from [26], the minimum-mean-squared-error (MMSE) equalizer from [19]–[21], and the Markov Chain Monte Carlo (MCMC) equalizer from [27]–[29], all of which can effectively utilize *a priori* information for data detection.

We conduct extensive tests on the progressive receiver using both simulations and experimental data from the Surface Processes and Acoustic Communications Experiment (SPACE08),

Manuscript submitted January 6, 2011, revised May 21, 2011, accepted June 10, 2011. This work was supported by the ONR grants N00014-07-1-0805 (YIP), N00014-09-1-0704 (PECASE) and the NSF grant CNS-0721834. This work was presented in part at the MTS/IEEE OCEANS conference, Sydney, Australia, May 24-27, 2010 [1]. The associate editor coordinating the review of this manuscript and approving it for publication was Dr. Geert Leus.

J.-Z. Huang, S. Zhou, J. Huang and P. Willett are with the Department of Electrical and Computer Engineering, University of Connecticut, Storrs, CT 06269, USA (e-mail: {jianzhong, shengli, jhuang, willett}@engr.uconn.edu).

C. R. Berger is with the Department of Electrical and Computer Engineering, Carnegie Mellon University, Pittsburgh, PA 15213, USA (e-mail: crberger@ece.cmu.edu).

Digital Object Identifier 00.0000/JSTSP.2011.0000000

conducted off the coast of Martha's Vineyard, MA, from Oct. 14 to Nov. 1, 2008. The reported experimental results include eight consecutive days, where the environmental conditions had significant changes. The progressive receiver achieves consistent performance despite large channel variations. In good channel conditions, it has as low complexity as the ICI-ignorant receiver in [2], [5]. In adverse channel conditions, it maintains excellent performance, but avoids the drawback of extra pilot overhead in the ICI-aware receiver as in [13]. Compared with an iterative receiver that uses a fixed ICI model, the proposed progressive receiver has comparable performance but much lower complexity.

The rest of this paper is organized as follows. Section II presents the system model and Section III describes the proposed progressive receiver in detail. Section V presents the simulation results and Section VI contains the experimental results. Section VII contains the conclusions.

Notation: Bold upper case and lower case letters denote matrices and column vectors, respectively; $(\cdot)^T$, $(\cdot)^*$, and $(\cdot)^H$ denote transpose, conjugate, and Hermitian transpose, respectively. $\mathbf{I}_N$ stands for an identity matrix with size N.

II. System Model

Zero-padded (ZP) OFDM is used as in [2], [3], [13]. Let T denote the OFDM symbol duration and T_g the guard interval. The total OFDM block duration is $T' = T + T_g$ and the subcarrier spacing is $1/T$. The kth subcarrier is at frequency

$$f_k = f_c + k/T,\ k = -K/2, \ldots, K/2-1, \tag{1}$$

where f_c is the carrier frequency and K subcarriers are used so that the bandwidth is $B = K/T$. Let $s[k]$ denote the information symbol to be transmitted on the kth subcarrier. The non-overlapping sets of active subcarriers $\mathcal{S}_A$ and null subcarriers $\mathcal{S}_N$ satisfy $\mathcal{S}_A \cup \mathcal{S}_N = \{-K/2, \cdots, K/2-1\}$. The transmitted passband signal is

$$\tilde{x}(t) = 2\mathrm{Re}\left\{ \left[\sum_{k\in\mathcal{S}_A} s[k] e^{j2\pi \frac{k}{T} t} g(t) \right] e^{j2\pi f_c t} \right\},\ t \in [0, T'] \tag{2}$$

where $g(t)$ is the pulse shaping filter whose Fourier transform is denoted by $G(f)$.

Assume that the UWA multipath channel consists of N_p discrete paths [13]

$$h(\tau, t) = \sum_{p=1}^{N_p} A_p(t) \delta\left(\tau - \tau_p(t)\right) \tag{3}$$

where $A_p(t)$ and $\tau_p(t)$ are the amplitude and delay of the pth path. Within the block duration T', we assume that i) the path amplitudes do not change $A_p(t) \approx A_p$, and ii) the path delays can be approximated by

$$\tau_p(t) = \tau_p - a_p t, \tag{4}$$

where τ_p is the delay at the start of the OFDM block and a_p is the Doppler rate corresponding to the pth path. As such, the channel model simplifies to

$$h(\tau, t) = \sum_{p=1}^{N_p} A_p \delta\left(\tau - (\tau_p - a_p t)\right), \tag{5}$$

and the passband signal at the receiver is

$$\tilde{y}(t) = \sum_{p=1}^{N_p} A_p \tilde{x}\left((1+a_p)t - \tau_p\right) + \tilde{v}(t), \tag{6}$$

where $\tilde{v}(t)$ is the additive noise.

As in [2], [13], the receiver applies a resampling operation to remove the dominant Doppler effect, which leads to a resampled passband signal $\tilde{z}(t) = \tilde{y}(t/(1+\hat{a}))$, where $1+\hat{a}$ is the resampling factor. Let $z(t)$ denote the baseband signal corresponding to $\tilde{z}(t)$. After the Doppler shift compensation $e^{-j2\pi\epsilon t}$ (see [2] for details on how to estimate ϵ), the FFT output on the mth subcarrier is

$$z[m] = \frac{1}{T} \int_0^{T+T_g} z(t) e^{-j2\pi\epsilon t} e^{-j2\pi \frac{m}{T} t}\, dt. \tag{7}$$

Plugging in $z(t)$ and carrying out the integration, we obtain:

$$z[m] = \sum_{p=1}^{N_p} \left(A_p^{'} e^{-j2\pi(f_m+\epsilon)\tau_p^{'}} \left(\sum_{k\in\mathcal{S}_A} \varrho_{m,k}(b_p) s[k] \right) \right) + v[m], \tag{8}$$

where $v[m]$ is the additive noise and

$$b_p = \frac{a_p - \hat{a}}{1+\hat{a}}, \quad A_p^{'} = \frac{A_p}{1+b_p}, \quad \tau_p^{'} = \frac{\tau_p}{1+b_p}, \tag{9}$$

$$\varrho_{m,k}(b_p) = G\left(f_m - f_k + \frac{\epsilon - b_p f_m}{1+b_p} \right). \tag{10}$$

With the definition of

$$H_{m,k} = \sum_{p=1}^{N_p} A_p^{'} e^{-j2\pi(f_m+\epsilon)\tau_p^{'}} \varrho_{m,k}(b_p) \tag{11}$$

we can rewrite the input-output relationship as

$$z[m] = \sum_{k\in\mathcal{S}_A} H_{m,k} s[k] + v[m]. \tag{12}$$

Clearly $H_{m,k}$ is the ICI coefficient that determines how the symbol transmitted on the kth subcarrier contributes to the output on the mth subcarrier. Using a matrix-vector notation, we can rewrite (12) as

$$\underbrace{\begin{pmatrix} z[-\frac{K}{2}] \\ \vdots \\ z[\frac{K}{2}-1] \end{pmatrix}}_{:=\mathbf{z}} = \underbrace{\begin{pmatrix} v[-\frac{K}{2}] \\ \vdots \\ v[\frac{K}{2}-1] \end{pmatrix}}_{:=\mathbf{v}} + \underbrace{\begin{pmatrix} H_{-\frac{K}{2},-\frac{K}{2}} & \cdots & H_{-\frac{K}{2},\frac{K}{2}-1} \\ \vdots & \ddots & \vdots \\ H_{\frac{K}{2}-1,-\frac{K}{2}} & \cdots & H_{\frac{K}{2}-1,\frac{K}{2}-1} \end{pmatrix}}_{:=\mathbf{H}} \underbrace{\begin{pmatrix} s[-\frac{K}{2}] \\ \vdots \\ s[\frac{K}{2}-1] \end{pmatrix}}_{:=\mathbf{s}} \tag{13}$$

where $\mathbf{z}$, $\mathbf{s}$, and $\mathbf{v}$ collect the FFT outputs, the transmitted data symbols, and the noise elements across all subcarriers $m = -K/2, -K/2+1, \ldots, K/2-1$, and $\mathbf{H}$ is the channel mixing matrix.

In [2] and [13], we have developed two block-by-block OFDM receivers based on different assumptions on the channel model:

- *ICI-ignorant receiver [2]*: It is assumed that all the paths have a similar Doppler rate $a_p = a, \forall p$, and hence the ICI can be ignored after proper resampling and Doppler shift compensation. As such, the channel mixing matrix $\mathbf{H}$ is diagonal, leading to low-complexity channel estimation and data demodulation. The experimental results in [2], [13] show that the ICI-ignorant receiver works well in good channel conditions, but its performance degrades considerably at adverse channel conditions.
- *ICI-aware receiver [13]*: It is assumed that all the paths have different Doppler rates, and hence ICI exists and is explicitly dealt with by the receiver. The ICI-aware receiver achieves excellent performance even in adverse channel conditions. However, a large number of pilots is needed for channel estimation, which reduces the spectral efficiency. Also, the complexity is much higher than that of ICI-ignorant receivers.

In this paper, we develop a progressive receiver structure that can adapt itself to channel conditions. It will have as low complexity as the ICI-ignorant receiver in good channel conditions, while achieving as excellent performance as the ICI-aware receiver in adverse channel conditions. Furthermore the progressive receiver does not require any extra pilot overhead, compared to the non-iterative receiver in [13].

III. Receiver Structure

We first present the overview of the proposed receiver structure in Section III-A, and then specify the key modules in Sections III-B – III-E.

A. The Progressive Receiver Structure

The proposed progressive receiver is an iterative receiver in nature, following the turbo principle. However, in contrast to existing iterative receivers in the literature, the system model used for channel identification and data demodulation changes at each iteration. It starts with a simple channel model that allows for ICI-ignorant receiver processing, and then progresses to ICI-aware receiver processing where the severity of the assumed ICI increases as the iteration goes on. The soft information obtained from the previous iteration contributes to channel estimation and data demodulation for the current iteration. This way, the receiver can self adapt to the "unknown" degree of channel variation progressively. The proposed receiver keeps the complexity low when the channel conditions are good, while still maintaining excellent performance when the channel conditions deteriorate.

The channel models used in the proposed receiver structure are parameterized by a parameter D as

$$H_{m,k} \simeq 0, \quad |m-k| > D. \tag{14}$$

In other words, each symbol only affects its D direct neighbors on each side, a reasonable assumption used in many existing works, e.g., [11], [22], [24], [30]. In this paper, we term D as the ICI depth and $2D+1$ as the ICI span. Let $\mathbf{H}_D$ denote the matrix carved from $\mathbf{H}$ keeping only the main diagonal and $2D$ off-diagonals, as shown in Fig. 1. The effective system model used for channel estimation and data demodulation is:

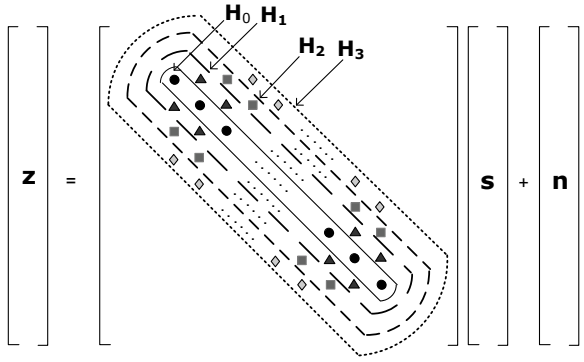

Fig. 1. The equivalent system model with different ICI spans.

$$\begin{aligned} \mathbf{z} &= \mathbf{H}_D\mathbf{s} + (\mathbf{H} - \mathbf{H}_D)\mathbf{s} + \mathbf{v} \\ &= \mathbf{H}_D\mathbf{s} + \mathbf{n}, \end{aligned} \tag{15}$$

where $\mathbf{n} := (\mathbf{H} - \mathbf{H}_D)\mathbf{s} + \mathbf{v}$ is the effective noise. In the proposed progressive receiver, the parameter D increases as the iteration goes on, and hence more severe ICI can be addressed as the receiver processing proceeds to deal with channels with large Doppler spread.

Fig. 2 depicts the progressive receiver structure, which consists of the following steps.

- *Step 1: Pre-processing.* For each received OFDM block, the receiver applies the pre-processing operation to remove the dominant Doppler effect [2]. Set $D = 0$.
- *Step 2: Channel estimation.* Estimate the equivalent channel mixing matrix $\mathbf{H}_D$ based on the assumed channel model given in (15).
- *Step 3: Noise variance estimation.* After channel estimation, the variance of the effective noise $\mathbf{n}$ is computed. This quantity is needed for ICI equalization.
- *Step 4: ICI equalization.* By using the estimated channel matrix $\mathbf{H}_D$, the equivalent noise variance, and the *a priori* information from the nonbinary LDPC decoder in the previous iteration, the ICI equalizer generates soft output on the reliability of the data symbols.
- *Step 5: Nonbinary LDPC decoding.* The nonbinary LDPC decoder yields the decoded information symbols and the soft information that can be used for channel estimation and ICI equalization [5]. During the decoding process, the decoder will declare success if all the parity check conditions are satisfied.
- *Step 6: Iteration among steps 2 to 5.* Increase D in the system model, and the assumed maximum Doppler spread of the channel to be estimated. Feed back the soft information to the channel estimator and the ICI equalizer. Iteration stops when the decoder declares a success, or when D reaches a pre-specified number $D_{\max}$.

In the proposed receiver as depicted in Fig. 2, each iteration is associated with a different D. The receiver can also iterate multiple times among step 2 to step 5 on channel estimation, equalization and decoding for each fixed D, before increasing

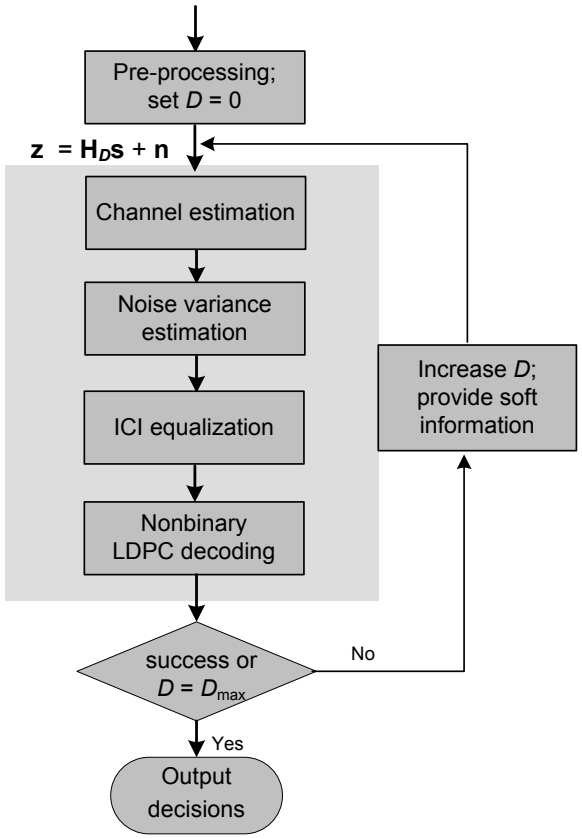

Fig. 2. Progressive receiver structure.

D to update the system model. Here we skip such a possibility for simplicity. Note that we have extended the progressive receiver structure to a multi-input multi-output (MIMO) system in [38], where multiple iterations among channel estimation, equalization and decoding are explicitly used for each system model with a particular D.

B. Sparse Channel Estimation

The inputs to the channel estimator are the observations in $\mathbf{z}$, the pilot symbols, and the *a posteriori* probabilities (APP) of the information symbols from the nonbinary LDPC decoder. Different strategies on how to use APP can be found in [9]. Here, we use the soft feedback strategy, which produces MMSE estimates of the information symbols as

$$\bar{s}[k] = \sum_{i=1}^{M} P_{\rm app}(s[k] = \alpha_i)\alpha_i, \quad \forall\ k \in \mathcal{S}_D \tag{16}$$

where M is the constellation size, α_i is the ith constellation point, $P_{\rm app}(\cdot)$ is the APP from LDPC decoder, and $\mathcal{S}_D$ is the set of data subcarriers in $\mathcal{S}_A$. Hence, an estimate of $\mathbf{s}$ (denoted by $\hat{\mathbf{s}}$) can be formed from

$$\hat{s}[k] = \begin{cases} s[k], & k \in \mathcal{S}_P, \\ 0, & k \in \mathcal{S}_N, \\ \bar{s}[k], & k \in \mathcal{S}_D, \end{cases} \tag{17}$$

where $\mathcal{S}_P$ is the set of pilot subcarriers from $\mathcal{S}_A$ ($\mathcal{S}_P \cup \mathcal{S}_D = \mathcal{S}_A$).

Despite having $K(2D+1)$ non-zero entries, the matrix $\mathbf{H}_D$ is determined by N_p triplets of (A'_p, b_p, τ'_p) as described in (11). Hence, instead of estimating the full channel matrix directly, we estimate the parameters of N_p channel paths. For sparse UWA channels [13], it is possible that these N_p paths can be identified based on only a limited number of measurements via advanced methods, such as compressed sensing. We will use the basis pursuit algorithms developed in the compressed sensing context as the building block [13].

The compressed sensing based channel estimator tries to identify the discrete paths from an overcomplete dictionary [13]. In particular, let us split the delay/Doppler ranges (τ', b) into a large number of dictionaries, and then connect the complex channel amplitudes with the frequency domain observations through the constructed dictionaries. On the delay and Doppler plane, a set of uniformly spaced points can be constructed from

$$\tau' \in \left\{0, \frac{T}{\lambda K}, \frac{2T}{\lambda K}, \ldots, \frac{(N_\tau - 1)T}{\lambda K}\right\}, \tag{18}$$

$$b^D \in \left\{-b^D_{\max}, -b^D_{\max} + \Delta b, \ldots, b^D_{\max}\right\}, \tag{19}$$

where the time resolution is chosen as a fraction, λ, of the baseband sampling time T/K, leading to $N_\tau = \lambda K T_g/T$ tentative delays. For the Doppler rates, we assume that they are spread around zero after pre-processing, and Δb is the Doppler resolution. $b^D_{\max}$ can be chosen based on the assumed Doppler spread for the current system model. There are

$$2b^D_{\max}/(\Delta b) + 1 = N^D_b, \tag{20}$$

tentative Doppler rates, leading to a delay-Doppler dictionary of size $N_\tau N^D_b$. During the iterations, the progressive receiver keeps the delay dictionary unchanged, but enlarges the Doppler dictionary size by increasing $b^D_{\max}$ as D increases. This way, channels with large Doppler spread can be addressed.

Let $\xi_{l,i}$ be the complex coefficient for a possible path that has delay τ'_l and Doppler scale b^D_i. Define a diagonal matrix $\mathbf{\Lambda}_l$ with $[\mathbf{\Lambda}_l]_{m,m} = e^{-j2\pi \frac{m}{T}\tau'_l}$. Define another matrix $\mathbf{\Gamma}^D_i$ having (m,k)th entry as

$$[\mathbf{\Gamma}^D_i]_{m,k} = \begin{cases} \varrho_{m,k}(b^D_i), & |m-k| \le D, \\ 0, & \text{otherwise}, \end{cases} \tag{21}$$

where $\varrho_{m,k}(\cdot)$ is defined in (10). Note that the Doppler template $\mathbf{\Gamma}^D_i$ is a banded matrix, corresponding to $\mathbf{H}_D$.

Therefore, the equivalent "mixing" channel matrix constructed by those $N_\tau N^D_b$ dictionaries can be written as

$$\mathbf{H}_D = \sum_{i=1}^{N^D_b} \sum_{l=1}^{N_\tau} \xi_{l,i} \mathbf{\Lambda}_l \mathbf{\Gamma}^D_i \tag{22}$$

With this, the observation $\mathbf{z}$ can be rewritten as the combi-

nation of all possible delay/Doppler dictionaries as

$$\begin{aligned}\mathbf{z} &= \mathbf{H}_D\hat{\mathbf{s}} + \mathbf{n} \\ &= \sum_{i=1}^{N_b^D}\sum_{l=1}^{N_\tau} \xi_{l,i}\mathbf{\Lambda}_l\mathbf{\Gamma}_i^D\hat{\mathbf{s}} + \mathbf{n} \\ &= \underbrace{[(\mathbf{\Lambda}_1\mathbf{\Gamma}_1^D\hat{\mathbf{s}}),\ \ldots,\ (\mathbf{\Lambda}_{N_\tau}\mathbf{\Gamma}_{N_b^D}^D\hat{\mathbf{s}})]}_{:=\mathbf{A}} \underbrace{\begin{bmatrix}\xi_{1,1}\\ \vdots \\ \xi_{N_\tau,N_b^D}\end{bmatrix}}_{:=\mathbf{x}} + \mathbf{n} \end{aligned} \quad (23)$$

Then, channel estimation becomes a fitting problem with the constraint that the solution $\mathbf{x}$ is sparse, which can be solved by the following convex optimization problem

$$\min_{\mathbf{x}} \|\mathbf{A}\mathbf{x} - \mathbf{z}\|^2 + \zeta \|\mathbf{x}\|_1, \quad (24)$$

where ζ is the regularization parameter to control the sparsity of $\mathbf{x}$.

After obtaining the sparse channel solution $\mathbf{x}$, we can reconstruct the frequency domain response according to (22). Many solvers for the formulation in (24) are available, see e.g., [31]–[33], but it should be noted that i) $\mathbf{x}$ is complex, and ii) the matrix $\mathbf{A}$ is of large dimension, but $\mathbf{Ab}$ and $\mathbf{A}^T\mathbf{c}$ can be evaluated efficiently. In this paper, we use the SpaRSA algorithm [34], which is based on iterative shrinkage/thresholding (IST). The complexity issue is investigated in [16].

Remark 1: During the first iteration, the symbol estimates from the decoder ([c.f. (24)]) are not available. Only the measurements on the pilot subcarriers are used for channel estimation, as done in [2]. Since only the delay grid is searched in the first iteration with $D = 0$, the number of measurements needed can be much smaller than the later iterations with $D > 0$.

Remark 2: We choose the sparsity factor ζ in (24) as a function of the effective signal-to-noise ratio (SNR) for each OFDM block as $\zeta = c/\sqrt{\text{SNR}}$, where c is a constant. In simulation and experimental results, c is set to 0.12. The effective SNR will be updated as the iteration goes on. Noise variance estimation is described in Section III-C.

C. Noise Variance Estimation

When D increases, more ICI will be modeled as opposed to being treated as additive noise. The variance of the effective noise hence needs to be updated at each iteration. We estimate the noise variance as

$$\hat{N}_0 = E\left[\left|z_m - \sum_{k=-D}^{k=D}\hat{H}_{m,m-k}\hat{s}[m-k]\right|^2\right], \quad (25)$$

where the expectation is carried out on the null subcarriers in $\mathcal{S}_N$ that are within the signal band. For $D = 0$, all the ICI terms are treated as additive noise, and $\hat{N}_0$ in (25) measures the energy on the null subcarriers [2]. As less ICI is viewed as additive noise, the effective signal-to-noise ratio (SNR) is expected to increase.

A simple noise-whitening approach as in [10] will be used when $D = 0$, as the effective noise may not be independent of the desired signal and ICI is the dominant source for the noise. As the iteration goes on with $D > 0$, the spillover from the neighboring subcarriers to the null subcarriers is extracted as in (25), and no whitening is applied.

D. ICI Equalization

After obtaining the estimated channel matrix $\hat{\mathbf{H}}_D$, the receiver now deals with ICI mitigation, based on the observations in $\mathbf{z}$ and the soft information (denoted by $\boldsymbol{\lambda}^e$) fed back from the nonbinary LDPC decoder.

Based on (15), the observation on the mth subcarrier can be written as

$$z[m] = \sum_{k=-D}^{k=D}\hat{H}_{m,m-k}s[m-k] + n[m], \quad (26)$$

which is in the convolution form but with coefficients that are changing from symbol to symbol. Hence, the ICI mitigation problem in the frequency domain is equivalent to an inter-symbol-interference (ISI) equalization problem in the time domain with time-varying channel taps. Existing methods for ISI equalization can be used for ICI equalization. Here we consider the MAP equalizer [26], the MMSE equalizer from [19], [20], and the Markov Chain Monte Carlo (MCMC) equalizer from [27]–[29], all of which can effectively incorporate soft information from the channel decoder.

1) MAP Equalizer: In our system with nonbinary LDPC codes, the size of the Galois field is matched to the constellation size, with each element in the finite field directly mapped to a constellation point [5]. The *a posteriori* log-likelihood-ratio vector (LLRV) for $s[m]$ is defined as $\boldsymbol{\lambda}[m] = [\lambda_0[m], \lambda_1[m], \ldots, \lambda_{M-1}[m]]^T$, where M is the constellation size and

$$\begin{aligned}\lambda_i[m] &= \ln\frac{P(s[m]=\alpha_i|\mathbf{z},\boldsymbol{\lambda}^e)}{P(s[m]=0|\mathbf{z},\boldsymbol{\lambda}^e)} \\ &= \ln\frac{\sum_{\mathbf{s}:s[m]=\alpha_i} P(\mathbf{z}|\mathbf{s},\boldsymbol{\lambda}^e)P(\mathbf{s}|\boldsymbol{\lambda}^e)}{\sum_{\mathbf{s}:s[m]=0} P(\mathbf{z}|\mathbf{s},\boldsymbol{\lambda}^e)P(\mathbf{s}|\boldsymbol{\lambda}^e)} \\ &= \ln\frac{\sum_{\mathbf{s}:s[m]=\alpha_i} P(\mathbf{z}|\mathbf{s})P(\mathbf{s}|\boldsymbol{\lambda}^e)}{\sum_{\mathbf{s}:s[m]=0} P(\mathbf{z}|\mathbf{s})P(\mathbf{s}|\boldsymbol{\lambda}^e)}\end{aligned} \quad (27)$$

The summation in the numerator and denominator of (27) are over a total of M^{K-1} combinations of $\mathbf{s}$. Due to the banded structure of $\mathbf{H}_m$, (27) can be expressed as (28), shown at the top of the next page. Hence, the correlation length among the postulated data sequence $\mathbf{s}$ is reduced from K to $2D$, and the well-known BCJR algorithm [35] can be used to evaluate (28), utilizing the ICI trellis structure.

2) MMSE Equalizer: An MMSE equalizer with *a priori* information from [19], [20] is used here for ICI mitigation. The channel decoder feeds back the extrinsic information, denoted as $\boldsymbol{\lambda}^e$, based on which the mean $\mu[k] := E(s[k])$ and the variance $\sigma^2[k] := \text{Cov}(s[k], s[k])$ can be calculated.

$$\lambda_i[m] = \ln \frac{\sum_{\mathbf{s}:s[m]=\alpha_i} \exp\left\{-\frac{1}{\hat{N}_0}\sum_{m=-K/2}^{K/2-1}\left|z[m]-\sum_{k=-D}^{k=D}\hat{H}_{m,m-k}s[m-k]\right|^2\right\} P(\mathbf{s}|\boldsymbol{\lambda}^e)}{\sum_{\mathbf{s}:s[m]=0} \exp\left\{-\frac{1}{\hat{N}_0}\sum_{m=-K/2}^{K/2-1}\left|z[m]-\sum_{k=-D}^{k=D}\hat{H}_{m,m-k}s[m-k]\right|^2\right\} P(\mathbf{s}|\boldsymbol{\lambda}^e)} \tag{28}$$

$$\underbrace{\begin{pmatrix} z[m-D] \\ \vdots \\ z[m+D] \end{pmatrix}}_{:=\mathbf{z}_m} = \underbrace{\begin{pmatrix} \hat{H}_{m-D,m-2D} & \cdots & \hat{H}_{m-D,m} & & \\ & \ddots & \vdots & \ddots & \\ & & \hat{H}_{m+D,m} & \cdots & \hat{H}_{m+D,m+2D} \end{pmatrix}}_{:=\hat{\mathbf{H}}_m} \underbrace{\begin{pmatrix} s[m-2D] \\ \vdots \\ s[m+2D] \end{pmatrix}}_{:=\mathbf{s}_m} + \underbrace{\begin{pmatrix} n[m-D] \\ \vdots \\ n[m+D] \end{pmatrix}}_{:=\mathbf{n}_m} \tag{29}$$

The a priori information for different symbols is assumed to be independent.

Based on (26), we collect the FFT outputs that are directly related to $s[m]$ as (29), shown at the top of this page. Now, let $\hat{\mathbf{h}}_m$ be the $(D+1)$th column of $\hat{\mathbf{H}}_m$:

$$\hat{\mathbf{h}}_m := \left[\hat{H}_{m-D,m}, \ldots, \hat{H}_{m+D,m}\right]^T, \tag{30}$$

which is of length $2D+1$. Define $\hat{\mathbf{H}}_m^-$ to be $\hat{\mathbf{H}}_m$ with $\hat{\mathbf{h}}_m$ removed, and $\mathbf{s}_m^-$ to be $\mathbf{s}_m$ with $s[m]$ removed. As such, we rewrite (29) as

$$\mathbf{z}_m = \hat{\mathbf{h}}_m s[m] + \hat{\mathbf{H}}_m^- \mathbf{s}_m^- + \mathbf{n}_m. \tag{31}$$

Based on the extrinsic information, define the mean and covariance of $\mathbf{s}_m^-$ as:

$$\boldsymbol{\mu}_m = E(\mathbf{s}_m^-), \quad \boldsymbol{\Sigma}_m = \mathrm{Cov}(\mathbf{s}_m^-, \mathbf{s}_m^-). \tag{32}$$

Note that no a priori information of $s[m]$ is included for the MMSE estimation of it, hence, $E(s[m])=0$ and $\sigma^2[m]=E_s$, where E_s is the average symbol energy. Further, the equivalent noise $\mathbf{n}$ is assumed Gaussian with a covariance matrix $\hat{N}_0\mathbf{I}$. The MMSE estimator for $s[m]$ based on (31) is then

$$\hat{s}[m] = \tag{33}$$
$$\hat{\mathbf{h}}_m^H\big[\hat{\mathbf{h}}_m\hat{\mathbf{h}}_m^H + \frac{\hat{N}_0}{E_s}\mathbf{I} + \frac{1}{E_s}\hat{\mathbf{H}}_m^-\boldsymbol{\Sigma}_m(\hat{\mathbf{H}}_m^-)^H\big]^{-1}(\mathbf{z}_m - \hat{\mathbf{H}}_m^-\boldsymbol{\mu}_m).$$

Assuming that $\hat{s}[m]$ is Gaussian distributed, the probabilities $P(\hat{s}[m]|s[m]=\alpha_i)$, $i=0,\ldots,M-1$, can be computed [19]. These probabilities are passed to the nonbinary LDPC decoder.

3) Markov Chain Monte Carlo (MCMC) Equalizer: The high complexity of the MAP equalizer lies in the exponential complexity in (28), where all the possible combinations within the correlation length are involved to calculate the LLRV of $s[m]$. In fact, only a handful of combinations, the *importance set*, contribute significantly to the summation in the numerator and denominator of (28). The MCMC method tries to find the *importance set* by browsing the possible choices of postulated data sequences in an efficient manner.

The MCMC method has been successfully applied for MIMO detection in [27], [28] and ISI equalization in [29]. It has been recently applied to UWA channels with single carrier transmission in [36]. Note that both bit-wise and group-wise MCMC detectors have been proposed [29]. Since there is no symbol-to-bit and bit-to-symbol conversion in our system, we now present the MCMC detector in a symbol-wise notation.

The procedure of MCMC sampling can be found in [27]–[29]. Assume that Ω importance samples are obtained after removing the redundant samples as in [27]. With the importance samples, the LLRV is computed as

$$\lambda_i[m] = \ln \frac{\sum_{n=1}^{\Omega} P(\mathbf{z}_m|\mathbf{s}_m^{-(n)}, s^{(n)}[m]=\alpha_i)P(\boldsymbol{\lambda}^e)}{\sum_{n=1}^{\Omega} P(\mathbf{z}_m|\mathbf{s}_m^{-(n)}, s^{(n)}[m]=0)P(\boldsymbol{\lambda}^e)}, \tag{34}$$

where $\mathbf{s}_m^{-(n)}$ is defined similar as in the MMSE equalizer based on the nth sample in Ω, and $P(\mathbf{z}_m|\mathbf{s}_m^{-(n)}, s^{(n)}[m]=\alpha_i)$ can be simplified as

$$P(\mathbf{z}_m|\mathbf{s}_m^{-(n)}, s^{(n)}[m]=\alpha_i) \sim \exp\left\{-\frac{1}{\hat{N}_0}\left\|\mathbf{z}_m - \hat{\mathbf{h}}_m\alpha_i - \hat{\mathbf{H}}_m^-\mathbf{s}_m^{-(n)}\right\|^2\right\}. \tag{35}$$

The main difference between the MCMC and the MAP equalizer is how large the contributing set Ω is. In the MAP equalizer, the size is M^{2D}, which is prohibitive to compute in practice for large M or D, while the MCMC equalizer only uses the importance set to approximate the optimal solution.

E. Nonbinary LDPC Decoding

Nonbinary LDPC decoding as in [5] is performed based on the equalizer outputs. The decoder outputs the decoded information symbols and the updated a posterior and extrinsic probabilities, which are used for the next round of channel estimation and data detection, respectively. During the decoding process, if all the parity check conditions are satisfied, the decoder declares success. This is a nice property associated with LDPC codes, which is well known in the coding literature.

IV. Discussion

A. Distinctions from Existing Iterative Receivers

The turbo principle has been recognized as one important methodology in advanced communication systems, and there is a large body of work on iterative receiver designs for wireless communications, see e.g. [21] and references therein.

One significant distinction of this work is that the system model keeps being updated during the iterations, while a fixed system model is usually assumed in existing iterative receivers [21]. This work is motivated by decoding the recorded data from experiments: practical underwater acoustic channels are constantly varying and the characteristics are largely affected by environmental conditions, and hence a fixed model would not be appropriate for all channel conditions.

B. Complexity of Channel Estimation

The complexity of sparse channel estimation in (24) depends on the the problem dimension. On the Dth iteration, N_b^D possible Doppler scaling factors are considered. For each tentative Doppler scale b_i^D, similar operations are carried out to evaluate the effects due to the path delays [16]. Hence, channel estimation complexity is approximately linear with N_b^D. In the problem studied in [16], the average runtime to solve (24) with $N_b^D = 15$ tentative Doppler rates is about 30 times larger than that with $N_b^D = 1$ for the ICI-ignorant receiver. Note that the proposed receiver gradually increases N_b^D during the iterations, which helps to lower the complexity.

C. Complexity of ICI Equalization

When D increases, the ICI equalization complexity increases at different rates for different equalizers.

- The complexity of a MAP equalizer is $O(M^{2D})$, which increases *exponentially* with D. Hence, the MAP equalizer is only suitable for small D and small constellation size M.
- The MMSE equalizer involves matrix inversion as in (33), and its complexity is cubic with D. Since D is small, the MMSE equalizer has low complexity. Further, the complexity does not depend on the constellation size M.
- The complexity of the MCMC equalizer depends on the sample size Ω and the constellation size M. Processing the probabilities in the log domain, the complexity of calculating (35) is $4D^2 + 5D$ complex multiplications (CMs) and $4D^2 + 5D$ complex additions (CAs). As the term $\hat{\mathbf{H}}_m^- \mathbf{s}_m^-$ in (35) is the same when drawing one particular symbol, the complexity of drawing samples for each symbol is roughly $\Omega(M(3D+1)+2D(2D+1))$ CMs and $\Omega(M(5D+2)+4D^2)$ CAs. Computing the output LLRVs as in (34) needs $\Omega(M(3D+1)+2D(2D+1))$ CMs and $\Omega(M(5D+2)+4D^2)$ CAs. Therefore, the total complexity for the MCMC equalizer is about $2\Omega K(M(3D+1)+2D(2D+1))$ CMs and $2\Omega K(M(5D+2)+4D^2)$ CAs. When $D < M$, the complexity is roughly linear with D.

V. Simulation Results

The system parameters are the same as used in the SPACE08 experiment, with bandwidth $B = 9.77$ kHz, symbol duration $T = 104.86$ ms, guard time $T_g = 24.6$ ms, and a rectangular pulse shaping filter[1]

$$g(t) = \begin{cases} 1, & t \in [0, T], \\ 0, & \text{otherwise.} \end{cases} \tag{36}$$

Out of $K = 1024$ subcarriers, there are 256 pilot subcarriers, 96 null subcarriers, and 672 data subcarriers. With rate 1/2 nonbinary LDPC coding, the data rate is

$$R = \frac{1}{2} \cdot \frac{672 \cdot \log_2 M}{T + T_g} = \begin{cases} 5.2 \text{ kb/s}, & \text{QPSK}, \\ 10.4 \text{ kb/s}, & \text{16-QAM}. \end{cases} \tag{37}$$

We generate sparse channels with $N_p = 15$ discrete paths, where the inter-arrival times are distributed exponentially with inter-arrival mean of 1 ms, leading to a total average delay spread of 15 ms. The amplitudes are Rayleigh distributed with the average power decreasing exponentially with delay. Each path has a separate Doppler rate, which is drawn from a uniform distribution with standard deviation of σ_v m/s. We choose a zero-mean Doppler distribution, as a non-zero mean could be removed through the resampling operation.

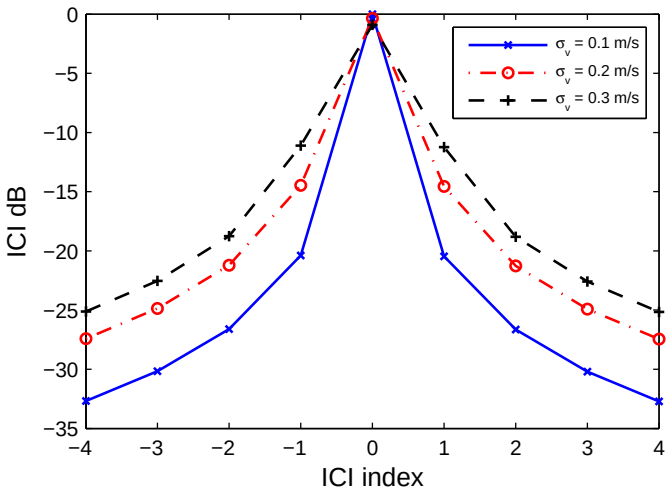

Fig. 3. Average ICI power $E\{|H_{m,m-D}|^2\}$ versus the ICI index D.

Fig. 3 plots $E\{|H_{m,m-D}|^2\}$ as a function of the ICI index D for various σ_v, normalized relative to $E\{|H_{m,m}|^2\}$. The ICI coefficients are calculated based on full channel state information (CSI). As expected, the average ICI power decreases as the ICI index increases. Most of symbol energy concentrates around the neighborhood of the desired subcarrier, while the ICI energy increases with σ_v. Hence, it becomes necessary to explicitly consider ICI when σ_v increases.

Figs. 4 and 5 show the performance of the progressive receiver with QPSK and 16-QAM constellations, respectively, where only one receive-phone is used. We use the block error rate (BLER) after LDPC decoding as the performance metric. The results are averaged over at least 1000 channel realizations or when 50 block errors are detected. The related

[1]Note that other pulse-shaping filters have been designed to improve the system performance in Doppler spread channels, e.g., [14], [15], [24]. However, their benefits have not yet been validated by experimental results. On the other hand, rectangular pulse-shaping filters have been extensively tested for multicarrier UWA communications [2], [3], [6], [7], [11], [12].

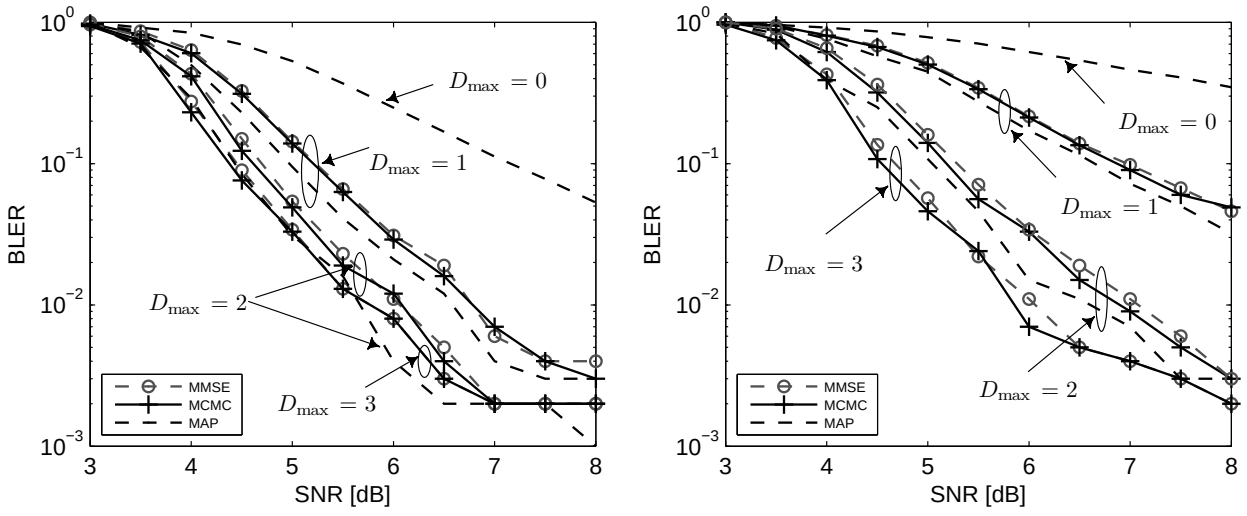

(a) $\sigma_v = 0.2$ m/s (b) $\sigma_v = 0.3$ m/s

Fig. 4. Simulated performance for the progressive receiver with different $D_{\max}$, QPSK.

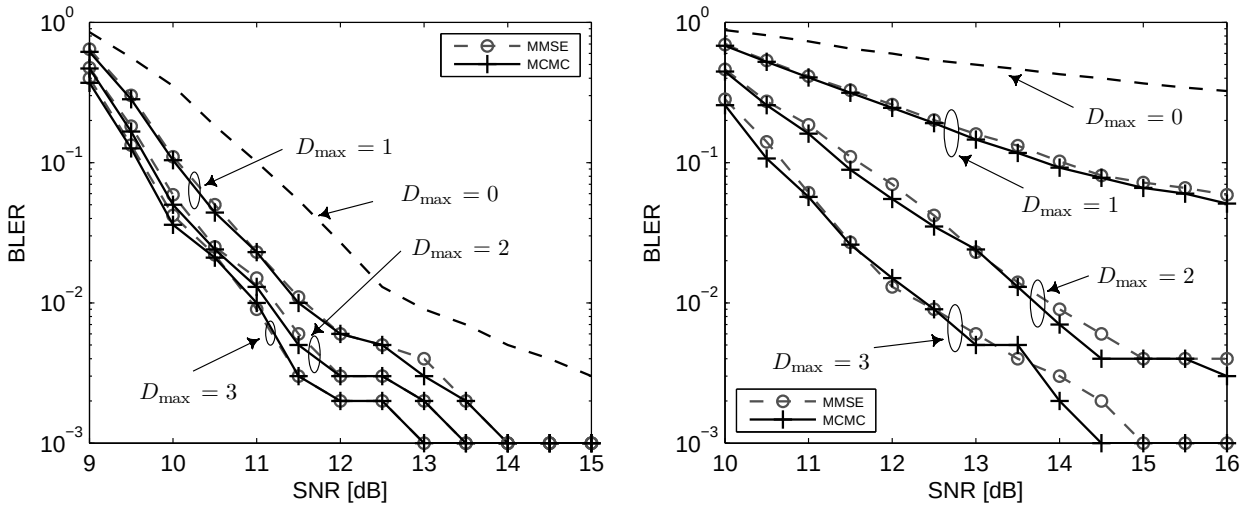

(a) $\sigma_v = 0.1$ m/s (b) $\sigma_v = 0.2$ m/s

Fig. 5. Simulated performance for the progressive receiver with different $D_{\max}$, 16-QAM.

parameters are $D_{\max} = 3$, the time resolution $\lambda = 2$ (as suggested in [13]), the Doppler resolution $\Delta b = 4 \cdot 10^{-5}$. As $\Delta b = \Delta v/c$, the corresponding velocity step size is $\Delta v = 0.06$ m/s. During the iteration process, $N_b^D = 7, 11$ and 15 for $D = 1$, 2 and 3, respectively. For the MCMC detector, we use $\Omega = 250$ samples with 5 parallel Gibbs samplers. Due to the high complexity, we only report the MAP equalization results for QPSK up to $D_{\max} = 2$. We can see that the MAP equalization outperforms the MMSE and MCMC slightly. The performance difference between MMSE and MCMC equalization is negligible, while both of them achieve significant performance improvement relative to the ICI-ignorant receiver.

We first consider 16-QAM with good channel conditions, see Fig. 5(a); at an operating SNR of 11 dB, more than 90% OFDM symbols can be decoded in the first round, i.e., using the ICI-ignorant receiver. Next we consider more adverse channel conditions as in Fig. 5(b). Clearly, the ICI-ignorant receiver now has very poor performance, decoding barely half of the OFDM symbols at 13 dB. In comparison, with $D_{\max} = 1$ about 80% of the OFDM symbols can be decoded, almost 97% at $D_{\max} = 2$, and more than 99% for $D_{\max} = 3$. This also means that only 20% of the time $D = 2$ has to be used and less than 3% of the time the algorithm runs to $D = 3$.

In the progressive receiver, the effective noise variance is re-estimated during each iteration, as shown in (25). Define the effective SNR as the energy ratio of the signal portion to the effective noise. Fig. 6 illustrates how the effective SNR changes during the progressive process across a certain range of SNR, where $\sigma_v = 0.3$ m/s and $\sigma_v = 0.2$ m/s for QPSK and 16-QAM, respectively. As more ICI is addressed, rather than

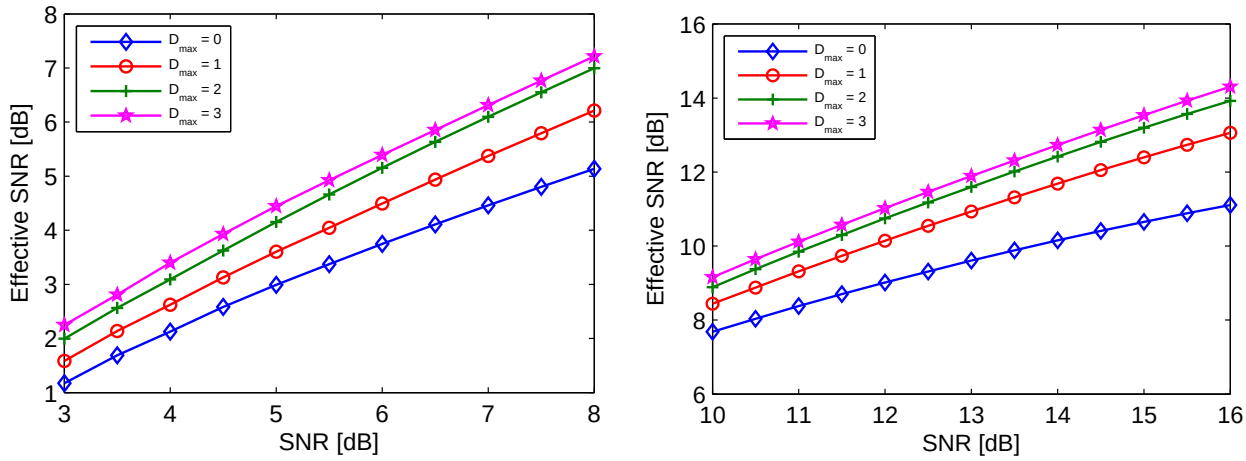

(a) $\sigma_v = 0.3$ m/s, QPSK (b) $\sigma_v = 0.2$ m/s, 16-QAM

Fig. 6. Estimated effective SNR during the progressive process. MMSE equalization.

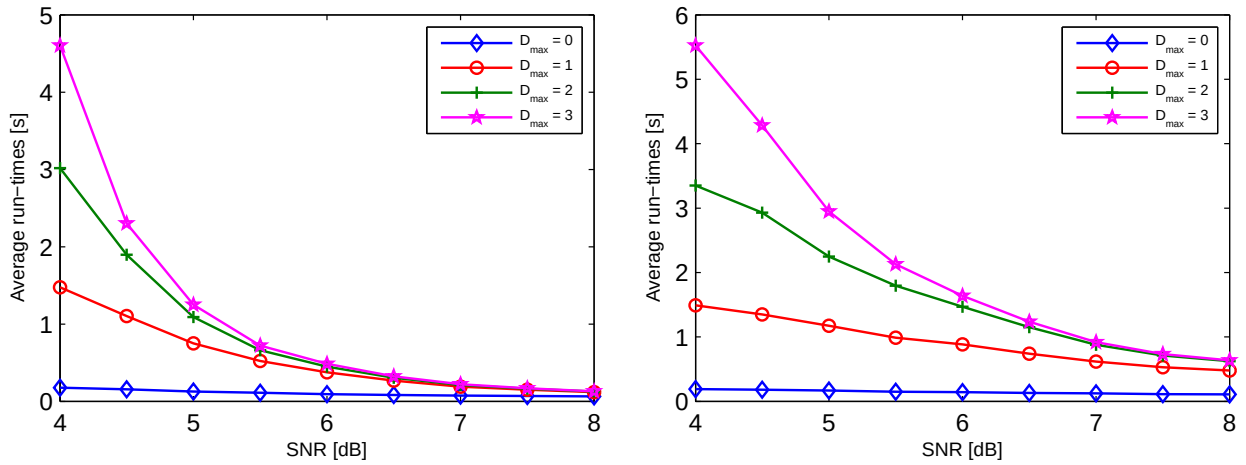

(a) $\sigma_v = 0.2$ m/s, QPSK (b) $\sigma_v = 0.3$ m/s, QPSK

Fig. 7. Average CPU run-times per OFDM block with the progressive receiver for different $D_{\max}$. MMSE equalization.

being regarded as additive noise, the effective SNR increases as the iteration goes on.

Now, let us briefly explore the complexity issue. Because both the sparse channel estimation and the LDPC decoding are iterative processes, which can stop at any time once the stopping criteria are met, we will not count the FLOPs of individual algorithms. Instead, we use the average receiver processing time per block for the proposed receiver. The numerical results were carried on under MATLAB 2007b, on a personal computer with an Intel(R) Core(TM)2 CPU 6600@2.4 GHz and 3GB of memory. A total of 10^4 OFDM blocks were tested for each SNR point. Fig. 7 shows the overall complexity of the progressive receiver for the setting of Fig. 4. In Fig. 7(a) when the channel conditions are good, the average total run-times for different $D_{\max}$ are close to the ICI-ignorant receiver at the medium to high SNR region. This verifies that the proposed receiver structure keeps the complexity low automatically when the channel conditions are good. In Fig. 7(b) corresponding to more challenging channels, the trend is similar that the average run-times decrease as the SNR improves. However, the complexity is larger than the ICI-ignorant receiver, as a large portion of OFDM blocks can only be recovered after explicit ICI mitigation. In this setting, the receiver complexity with $D_{\max} = 2, 3$ converges to that of $D_{\max} = 1$ at high SNR, suggesting that the $D = 2$ and $D = 3$ iterations are used infrequently.

The progressive receiver needs to implement all the functions of different D values. However, the progressive receiver will likely be run on software-defined modems [37], where storage is not a concern. Rather, the processing speed is the main focus in order to meet real-time data processing requirements.

VI. Experimental Results

We use data recorded during the SPACE08, conducted off the coast of Martha's Vineyard, MA, from Oct. 14 to Nov. 1, 2008. The water depth was about 15 meters, the transmitter was approximately 4 meters from the sea floor, and the top of the receive arrays were about 3.25 meters above the sea floor, as shown in Fig. 8.

TABLE I
THE NUMBER OF UNDECODED OFDM BLOCKS FOR DIFFERENT VALUES OF $D_{\max}$ IN THE PROGRESSIVE RECEIVER. JULIAN DATES 295-302. 16-QAM, RATE 1/2 CODING, MMSE BASED ICI EQUALIZATION

System	S1 (60 m); 1560 blocks				S3 (200 m); 1640 blocks				S5 (1000 m); 1600 blocks			
# of Phones	$D_{\max}$=0	1	2	3	$D_{\max}$=0	1	2	3	$D_{\max}$=0	1	2	3
1	1178	1048	951	877	1229	1141	1090	1046	809	758	743	732
2	731	565	431	298	775	679	630	583	395	337	296	277
3	350	215	123	73	470	368	299	259	179	136	119	104
4	152	77	38	19	213	126	80	57	109	86	76	66
5	70	32	13	5	88	47	24	15	82	65	51	37
6	36	19	8	4	44	17	9	8	68	46	30	23
7	24	12	6	2	16	9	4	0	53	34	21	18
8	19	10	4	1	11	3	0	0	45	22	14	12
9	16	7	3	0	4	2	0	0	37	19	14	13
10	13	6	2	0	2	0	0	0	26	16	14	13
11	11	5	2	0	0	0	0	0	25	17	11	11
12	9	5	2	0	0	0	0	0	23	12	10	9

TABLE II
THE NUMBER OF UNDECODED OFDM BLOCKS FOR DIFFERENT VALUES OF $D_{\max}$ IN THE PROGRESSIVE RECEIVER. JULIAN DATES 295-302. 16-QAM, RATE 1/2 CODING, MCMC BASED ICI EQUALIZATION

System	S1 (60 m); 1560 blocks				S3 (200 m); 1640 blocks				S5 (1000 m); 1600 blocks			
# of Phones	$D_{\max}$=0	1	2	3	$D_{\max}$=0	1	2	3	$D_{\max}$=0	1	2	3
1	1178	1041	933	855	1229	1136	1078	1034	809	758	741	727
2	731	556	397	281	775	673	619	563	395	333	291	265
3	350	202	112	60	470	365	288	242	179	136	114	103
4	152	75	33	16	213	120	72	48	109	85	71	60
5	70	31	11	4	88	42	21	12	82	64	42	30
6	36	19	6	3	44	16	9	5	68	43	24	23
7	24	11	5	2	16	9	3	1	53	30	18	17
8	19	9	4	0	11	3	0	0	45	20	12	10
9	16	7	2	0	4	1	0	0	37	17	13	12
10	13	7	2	0	2	0	0	0	26	16	12	12
11	11	5	2	0	0	0	0	0	25	16	11	11
12	9	5	2	0	0	0	0	0	23	11	10	10

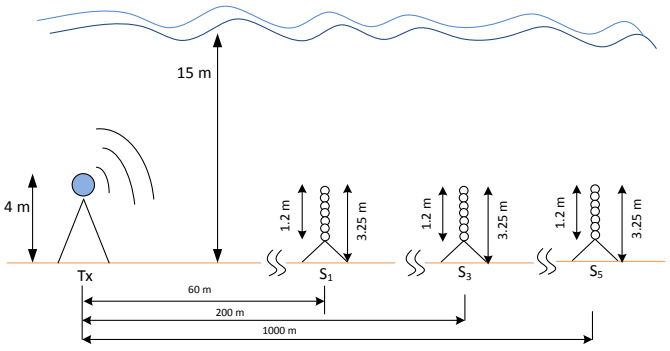

Fig. 8. Setup of SPACE08 experiment.

The carrier frequency was $f_c = 13$ kHz, and the sampling frequency was $f_s = 39.0625$ kHz. More experiment descriptions can be found in [13], [18]. A transmission occurred every two hours, resulting in 12 recorded files each day. For each transmission, there are 20 OFDM blocks with the parameters specified in the simulation settings. Hence, the data rate is 10.4 kb/s, with 16-QAM and rate-1/2 nonbinary LDPC coding over a bandwidth of 9.77 kHz.

We report performance results for Julian dates 295 – 302 (Oct. 21 – 28) and consider three receivers, labeled as S1, S3, and S5, which were 60 m, 200 m, and 1,000 m from the transmitter, respectively. The Doppler resolution and the dictionary size are the same as used in the simulation. The typical channel responses for SPACE08 experiment can be found in [13, Fig. 10].

A. Performance Overview

Tables I and II report the number of OFDM blocks that *have not been decoded correctly* as D increases in the progressive receiver, using the MMSE and MCMC equalizers, respectively, with different number of phones combined[2]. The data across eight days (Julian dates 295-302) is used. Since some recorded files are corrupted, there are a total of 1560, 1640 and 1600 blocks processed for S1, S3 and S5, respectively. Comparing Tables I and II, we see that the MCMC equalizer performs slightly better when only a small number of hydrophones are combined, and the gap closes when more hydrophones are available. Combining 12 hydrophones, *all blocks* in S1 and S3 are decoded correctly using the progressive receiver when it reaches $D = 3$. There are 9 (with MMSE) or 10 (with MCMC) blocks that cannot be decoded in S5. Since the performance difference between MMSE and MCMC is small, in the following we use the MMSE results for illustration.

[2]For recorded data, one common practice is to investigate the performance as a function of the number of phones combined. Note that with more phones, the SNR after combining increases, hence performance improvement is due to both diversity effect and SNR increase. In this paper, the phones are selected sequentially across the array, from top to the bottom. The frequency domain observations are stacked into a longer vector to the equalizer. The extension from single channel processing to multichannel processing is straightforward. See also [38] for the extension to MIMO equalization.

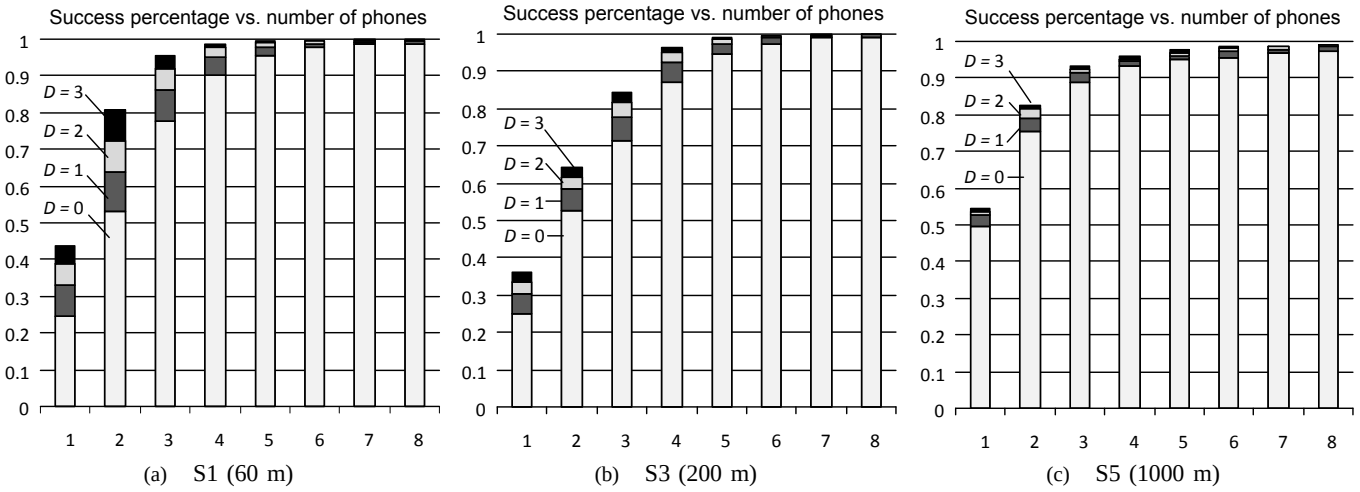

Fig. 9. The block success percentage averaged over Julian dates 295-302, SPACE08, MMSE based ICI equalization.

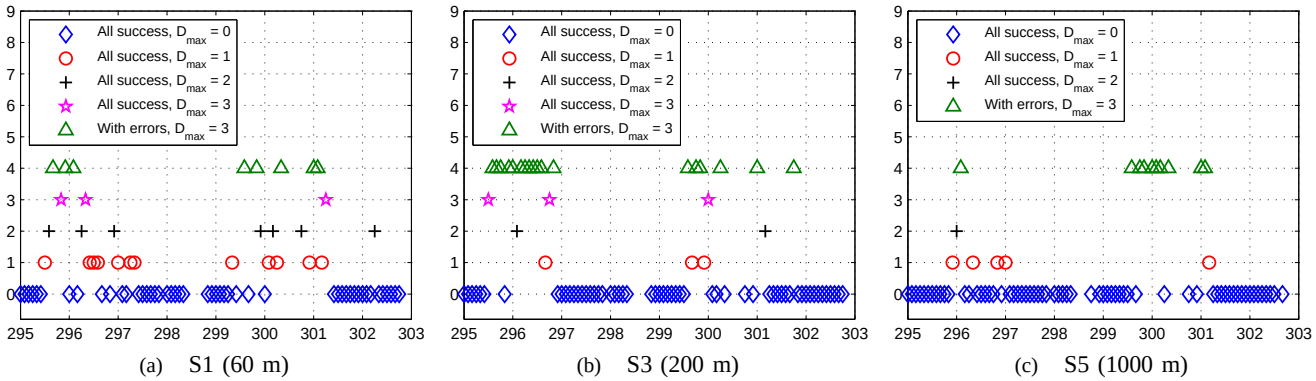

Fig. 10. Success level for each transmission of 20 OFDM blocks; four hydrophones. Markers are placed at convenient heights for illustration purposes only.

Fig. 9 shows the block success rate averaged over the eight consecutive days using the proposed progressive receiver with the MMSE equalizer. At short (S1) to medium (S3) ranges, we expect rich multipath and significant Doppler variation due to the geometry. When the number of hydrophones is small, the performance of the ICI-ignorant receiver ($D = 0$) is limited, and many more OFDM symbols can be decoded by applying the progressive procedure, with a larger D. When the number of hydrophones is large, the ICI-ignorant receiver already achieves excellent results for all the blocks. Checking the results using four hydrophones, about 90% OFDM blocks can be decoded at the $D = 0$ stage, and the success rate increases to 95% when $D_{\max} = 1$, and up to 98.8% when $D_{\max} = 3$.

For S5, we see similar trends as S1 and S3, but the gap between the ICI-ignorant and progressive receivers gets smaller. When four hydrophones are combined, over 93% blocks can be decoded by ignoring the ICI, and the success rate increases to 96% when the progressive receiver reaches $D = 3$.

B. Environmental Impact

Using four hydrophones for combining, Table I shows that there are 19 out of 1560 blocks with decoding errors in S1, 57 out of 1640 blocks with decoding errors in S3, and 66 out of 1600 blocks with decoding errors in S5, for the progressive receiver with $D_{\max} = 3$. Fig. 10 illustrates the success level of each transmission of 20 OFDM blocks across the 8-day period. Each day, we have about 12 files recorded (a few files are corrupted). "All success" means that all 20 blocks in that file, of duration $20(T + T_g) = 2.59$ s, can be decoded, while "With errors" means that some blocks cannot be decoded out of 20 blocks in the file.

The significant wave height and average wind speed are shown in Fig. 11. The significant wave height is calculated as $H = 4\sqrt{m_0}$, where m_0 is the zeroth-moment of the variance spectrum obtained by integration of the variance spectrum. We can observe some correlations between Fig. 10 and Fig. 11. There are two periods that the progressive receiver with $D > 0$ is used: Julian dates 296-297 and Julian dates 300-301, during which the wind speed and the wave height are high. For the rest of the days, the ICI-ignorant receiver can decode all the blocks. Fig. 10 confirms that the progressive receiver can self adapt to channel conditions, maintaining both good performance and low complexity.

C. Progressive versus Iterative ICI-aware receivers

In Fig. 12, we compare the performance between the proposed progressive receiver and an iterative ICI-aware re-

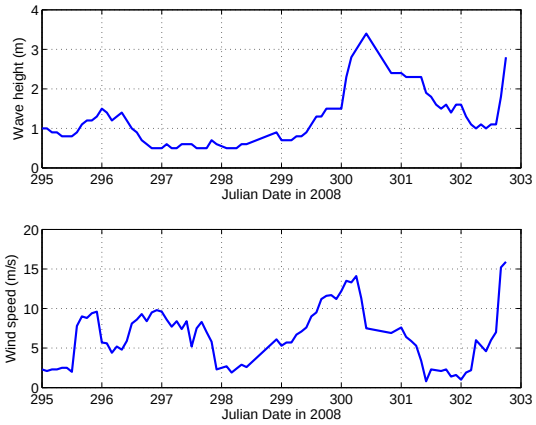

Fig. 11. Significant wave height and average wind speed for selected days in SPACE08.

ceiver that fixes the channel model at $D = 3$, but iterates several times; we focus on channels with large Doppler spread (Julian Date 300). Obviously, the latter receiver has much higher complexity, and is not well-motivated in good channel conditions. After the first iteration, we see that the ICI-aware receiver outperforms the ICI-ignorant receiver. As the iteration continues, the progressive receiver catches up with the iterative ICI-aware receiver, and the performance difference is negligible. Hence, the progressive receiver collects the performance benefits as the iterative ICI-aware receiver, but enjoys much lower complexity in various channel conditions.

VII. Conclusions

In this paper we developed a progressive receiver for OFDM transmission over time-varying underwater acoustic channels. During the iterations, it updates the *system model* to account for channels with large Doppler spreads, while fully utilizing soft information from the previous iteration for enhanced sparse channel estimation and inter-carrier interference equalization. Extensive tests based on experimental data showed that the proposed receiver enjoys low complexity in good channel conditions while maintaining excellent performance even when the channel deteriorates. Adapting to channel variations without any *a priori* information, the proposed receiver is very promising for practical underwater systems.

Acknowledgement

We thank Dr. James Preisig and his team for conducting the SPACE08 experiment.

References

[1] J.-Z. Huang, S. Zhou, J. Huang, C. R. Berger, and P. Willett, "Progressive inter-carrier interference equalization for OFDM transmission over time-varying underwater acoustic channels," in *Proc. of MTS/IEEE OCEANS Conf.*, Sydney, Australia, May 2010.

[2] B. Li, S. Zhou, M. Stojanovic, L. Freitag, and P. Willett, "Multicarrier communication over underwater acoustic channels with nonuniform Doppler shifts," *IEEE J. Ocean. Eng.*, vol. 33, no. 2, pp. 198–209, Apr. 2008.

[3] M. Stojanovic, "Low complexity OFDM detector for underwater channels," in *Proc. of MTS/IEEE OCEANS Conf.*, Boston, MA, Sept. 18-21, 2006.

[4] ——, "OFDM for underwater acoustic communications: Adaptive synchronization and sparse channel estimation," in *Proc. of Intl. Conf. on Acoustics, Speech and Signal Proc.*, Las Vegas, NV, Mar. 30 – Apr. 4, 2008.

[5] J. Huang, S. Zhou, and P. Willett, "Nonbinary LDPC coding for multicarrier underwater acoustic communication," *IEEE J. Select. Areas Commun.*, vol. 26, no. 9, pp. 1684–1696, Dec. 2008.

[6] T. Kang and R. A. Iltis, "Iterative carrier frequency offset and channel estimation for underwater acoustic OFDM systems," *IEEE J. Select. Areas Commun.*, vol. 26, no. 9, pp. 1650–1661, Dec. 2008.

[7] Y. Emre, V. Kandasamy, T. M. Duman, P. Hursky, and S. Roy, "Multi-input multi-output OFDM for shallow-water UWA communications," in *Acoustics'08 Conference*, Paris, France, July 2008.

[8] B. Li, J. Huang, S. Zhou, K. Ball, M. Stojanovic, L. Freitag, and P. Willett, "MIMO-OFDM for high rate underwater acoustic communications," *IEEE J. Ocean. Eng.*, vol. 34, no. 4, pp. 634–644, Oct. 2009.

[9] J. Huang, J.-Z. Huang, C. R. Berger, S. Zhou, and P. Willett, "Iterative sparse channel estimation and decoding for underwater MIMO-OFDM," *EURASIP Journal on Advances in Signal Processing.*, vol. 2010, article ID 460379.

[10] C. R. Berger, W. Chen, S. Zhou, and J. Huang, "A Simple and Effective Noise Whitening Method for Underwater Acoustic Orthogonal Frequency Division Multiplexing," *Journal of Acoustical Society of America*, vol. 127, no. 4, pp. 2358-2367, April 2010.

[11] G. Leus and P. A. van Walree, "Multiband OFDM for covert acoustic communications," *IEEE J. Select. Areas Commun.*, vol. 26, no. 9, pp. 1662–1673, Dec. 2008.

[12] K. Tu, D. Fertonani, T. M. Duman, and P. Hursky, "Mitigation of intercarrier interference in OFDM systems over underwater acoustic channels," in *Proc. of MTS/IEEE OCEANS Conf.*, Bremen, Germany, May. 2009.

[13] C. R. Berger, S. Zhou, J. Preisig, and P. Willett, "Sparse channel estimation for multicarrier underwater acoustic communication: From subspace methods to compressed sensing," *IEEE Trans. Signal Processing*, vol. 58, no. 3, pp. 1708 – 1721, Mar. 2010.

[14] W. Kozek, and A. F. Molisch, "Nonorthogonal pulse shapes for multicarrier communications in doubly dispersive channels," *IEEE Journal on selected areas in communications.*, vol. 16, no. 8, pp. 1579-1589, Oct. 1998.

[15] T. Strihmer, and S. Beaver, "Optimal OFDM design for time-frequency dispersive channels," *IEEE Transactions on communications.*, vol. 51, no. 7, pp. 1-12, July. 2003.

[16] J.-Z. Huang, C. R. Berger, S. Zhou, and J. Huang, "Comparison of basis pursuit algorithms for sparse channel estimation in underwater acoustic OFDM," in *Proc. of MTS/IEEE OCEANS Conf.*, Sydney, Australia, May. 2010.

[17] A. Song, M. Badiey, H.-C. Song, W. S. Hodgkiss, M. B. Porter, and the KauaiEx Group, "Impact of ocean variability on coherent underwater acoustic communications during the Kauai experiment (KauaiEx)," *J. Acoustical Society of America.*, vol. 123, no. 2, pp. 856–865, Feb. 2008.

[18] L. Freitag and S. Singh, "Performance of micro-modem PSK signalling under variable conditions during the 2008 RACE and SPACE experiments," in *Proc. of MTS/IEEE OCEANS Conf.*, Biloxi, MS, Oct. 2009.

[19] M. Tüchler, A. C. Singer, and R. Koetter, "Minimum mean squared error

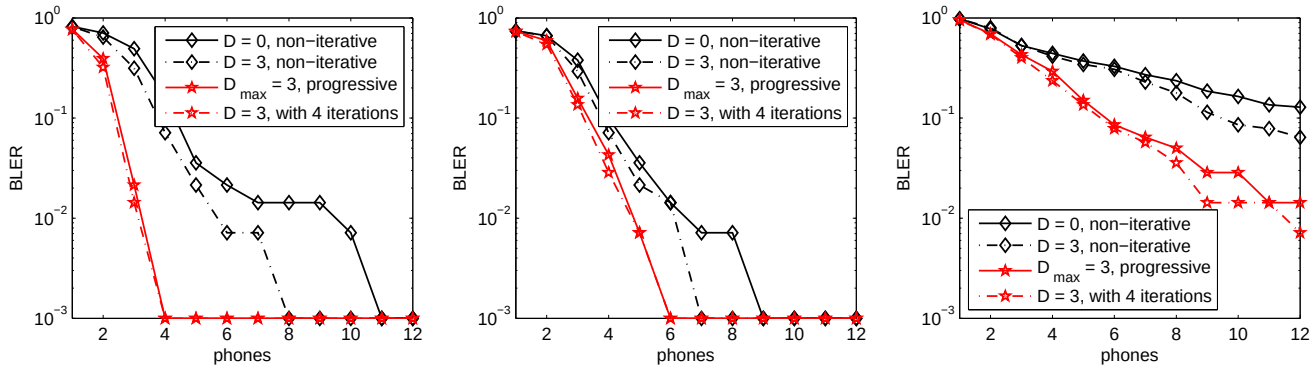

(a) S1 (60 m) (b) S3 (200 m) (c) S5 (1000 m)

Fig. 12. Performance comparisons between progressive and iterative ICI-aware receivers; Julian date 300.

equalization using a priori information," *IEEE Trans. Signal Processing*, vol. 50, no. 3, pp. 673–683, Mar. 2002.

[20] M. Tüchler, R. Koetter, and A. C. Singer, "Turbo equalization: Principles and new results," *IEEE Trans. Commun.*, vol. 50, no. 5, pp. 754–767, May. 2002.

[21] R. Koetter, A. C. Singer, and M. Tüchler, "Turbo equalization," *IEEE Signal Processing Magazine*, vol. 21, no. 1, pp. 67–80, Jan. 2004.

[22] L. Rugini, P. Banelli, and G. Leus, "Simple equalization of time-varying channels for OFDM," *IEEE Commun. Lett.*, vol. 9, no. 7, pp. 619–621, July. 2005.

[23] L. Rugini, P. Banelli, and G. Leus, "Low-complexity banded equalizers for OFDM systems in Doppler spread channels," *EURASIP J. Appl. Signal Processing.*, vol. 2006, pp. 1–13, 2006.

[24] S. J. Hwang and P. Schniter, "Efficient multicarrier communication for highly spread underwater acoustic channels," *IEEE J. Select. Areas Commun.*, vol. 26, no. 9, pp. 1674–1683, Dec. 2008.

[25] D. N. Liu and M. P. Fitz, "Iterative MAP equalization and decoding in wireless mobile coded OFDM," *IEEE Trans. Commun.*, vol. 57, no. 7, pp. 2042–2051, July. 2009.

[26] C. Douillard, M. Jezequel, C. Berrou, A. Picart, P. Didier, and A. Glavieux, "Iterative correction of intersymbol interference: Turbo equalization," *European Trans. on Telecomm.*, vol. 6, 1995.

[27] B. Farhang-Boroujeny, H. Zhu, and Z. Shi, "Markov chain Monte Carlo algorithms for CDMA and MIMO communication systems," *IEEE Trans. Signal Processing*, vol. 54, no. 5, pp. 1896–1909, May. 2006.

[28] R.-R. Chen, R. Peng, B. Farhang-Beroujeny, and A. Ashikhmin, "Approaching MIMO capacity using bitwise Markov chain Monte Carlo detection," *IEEE Trans. Commun.*, vol. 58, no. 2, pp. 423–428, Feb. 2010.

[29] R. Peng, R.-R. Chen, and B. Farhang-Beroujeny, "Markov chain Monte Carlo detectors for channels with intersymbol interference," *IEEE Trans. Signal Processing*, vol. 58, no. 4, pp. 2206–2217, Apr. 2010.

[30] W. G. Jeon and K. H. Chang, "An equalization technique for orthogonal frequency-division multiplexing systems in time-variant multipath channels," *IEEE Trans. Commun.*, vol. 47, no. 1, pp. 27–32, Jan. 1999.

[31] S.-J. Kim, K. Koh, M. Lustig, S. Boyd, and D. Gorinevsky, "An interior-point method for large-scale l_1-regularized least squares," *IEEE J. Select. Topics Signal Proc.*, vol. 1, no. 4, pp. 606–617, Dec. 2007.

[32] M. A. T. Figueiredo, R. D. Nowak, and S. J. Wright, "Gradient projection for sparse reconstruction: Application to compressed sensing and other inverse problems," *IEEE J. Select. Topics Signal Proc.*, vol. 1, no. 4, pp. 586–597, Dec. 2007.

[33] J. Yang and Y. Zhang, "Alternating direction algorithms for l_1 problems in compressive sensing," Rice Univ., Houston, TX, CAAM Tech. Rep. TR09-37, 2009; available at http://www.caam.rice.edu/˜optimization/L1/.

[34] S. J. Wright, R. D. Nowak, and M. A. T. Figueiredo, "Sparse reconstruction by separable approximation," *IEEE Trans. Signal Processing*, vol. 57, no. 7, pp. 2479–2493, Jul. 2009.

[35] L. R. Bahl, J. Cocke, F. Jelinek, and J. Raviv, "Optimal decoding of linear codes for minimizing symbol error rate," *IEEE Trans. Inform. Theory*, vol. 20, pp. 284–287, Mar. 1974.

[36] H. Wan, R.-R. Chen, J. W. Choi, A. Singer, J. Preisig, and B. Farhang-Boroujeny, "Markov chain Monte Carlo detection for underwater acoustic channels," in *Proc. Information theory and applications workshop (ITA)*, 2010.

[37] H. Yan, S. Zhou, Z. Shi, J.-H. Cui, L. Wan, J. Huang, and H. Zhou, "DSP implementation of SISO and MIMO OFDM acoustic modems," in *Proc. of MTS/IEEE OCEANS Conference*, Sydney, Australia, May 24–27, 2010.

[38] J.-Z. Huang, S. Zhou, J. Huang, J. Preisig, L. Freitag, and P. Willett, "Progressive MIMO-OFDM reception over time-varying underwater acoustic channels," in *Proc. of the 44th Asilomar Conf. on Signals, Systems, and Computers*, Pacific Grove, CA, Nov. 2010.

Jianzhong Huang (S'09) received his B.S. degree in 2003 and his M.Sc. degree in 2006, from Xidian University, Xi'an, Shaanxi China, both in communication engineering. He is currently working toward his Ph.D. degree in the Department of Electrical and Computer Engineering at the University of Connecticut, Storrs. His research interests lie in the areas of communications and signal processing, currently focusing on multicarrier modulation algorithms and channel coding for underwater acoustic communications.

Shengli Zhou (M'03) received the B.S. degree in 1995 and the M.Sc. degree in 1998, from the University of Science and Technology of China (USTC), Hefei, both in electrical engineering and information science. He received his Ph.D. degree in electrical engineering from the University of Minnesota (UMN), Minneapolis, in 2002.

He has been an assistant professor with the Department of Electrical and Computer Engineering at the University of Connecticut (UCONN), Storrs, 2003-2009, and now is an associate professor. He holds a United Technologies Corporation (UTC) Professorship in Engineering Innovation, 2008-2011. His general research interests lie in the areas of wireless communications and signal processing. His recent focus is on underwater acoustic communications and networking.

Dr. Zhou served as an associate editor for IEEE Transactions on Wireless Communications, Feb. 2005 – Jan. 2007, and IEEE Transactions on Signal Processing, Oct. 2008 – Oct. 2010. He is now an associate editor for IEEE Journal of Oceanic Engineering. He received the 2007 ONR Young Investigator award and the 2007 Presidential Early Career Award for Scientists and Engineers (PECASE).

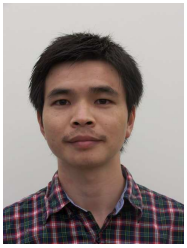

Jie Huang received the B.S. degree in 2001 and the Ph. D. degree in 2006, from the University of Science and Technology of China (USTC), Hefei, both in electrical engineering and information science. He was a post-doctoral researcher with the Department of Electrical and Computer Engineering at the University of Connecticut (UCONN), Storrs, from July 2007 to June 2009, and is now a research assistant professor at the University of Connecticut (UCONN), Storrs.

His general research interests lie in the areas of communications and signal processing, specially error control coding theory and coded modulation. His recent focus is on signal processing, channel coding and network coding for underwater acoustic communications and networks.

Christian R. Berger (M'09) was born in Heidelberg, Germany, on September 12, 1979. He received the Dipl.-Ing. degree from the Universität Karlsruhe (TH), Karlsruhe, Germany in 2005, and the Ph.D. degree from the University of Connecticut, Storrs, in 2009, both in electrical engineering.

In the summer of 2006, he was as a visiting scientist at the Sensor Networks and Data Fusion Department of the FGAN Research Institute, Wachtberg, Germany. He is currently a post-doctoral researcher at the Department of Electrical and Computer Engineering, Carnegie Mellon University, Pittsburgh, USA. His research interests lie in the areas of communications and signal processing, including distributed estimation in wireless sensor networks, wireless positioning and synchronization, underwater acoustic communications and networking.

Dr. Berger has served as a reviewer for the IEEE Transactions on Signal Processing, Wireless Communications, Vehicular Technology, and Aerospace and Electronic Systems. In 2008 he was member of the technical program committee and session chair for the 11th International Conference on Information Fusion in Cologne, Germany.

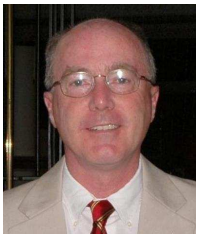

Peter Willett (F'03) received his BASc (Engineering Science) from the University of Toronto in 1982, and his PhD degree from Princeton University in 1986.

He has been a faculty member at the University of Connecticut ever since, and since 1998 has been a Professor. His primary areas of research have been statistical signal processing, detection, machine learning, data fusion and tracking. He has interests in and has published in the areas of change/abnormality detection, optical pattern recognition, communications and industrial/security condition monitoring.

Dr. Willett is editor-in-chief for IEEE Transactions on Aerospace and Electronic Systems, and until recently was associate editor for three active journals: IEEE Transactions on Aerospace and Electronic Systems (for Data Fusion and Target Tracking) and IEEE Transactions on Systems, Man, and Cybernetics, parts A and B. He is also associate editor for the IEEE AES Magazine, editor of the AES Magazines periodic Tutorial issues, associate editor for ISIFs electronic Journal of Advances in Information Fusion, and is a member of the editorial board of IEEEs Signal Processing Magazine. He has been a member of the IEEE AESS Board of Governors since 2003. He was General Co- Chair (with Stefano Coraluppi) for the 2006 ISIF/IEEE Fusion Conference in Florence, Italy, Program Co-Chair (with Eugene Santos) for the 2003 IEEE Conference on Systems, Man, and Cybernetics in Washington DC, and Program Co-Chair (with Pramod Varshney) for the 1999 Fusion Conference in Sunnyvale.